Comrie et al., http://www.jcb.org/cgi/content/full/jcb.201406120/DC1

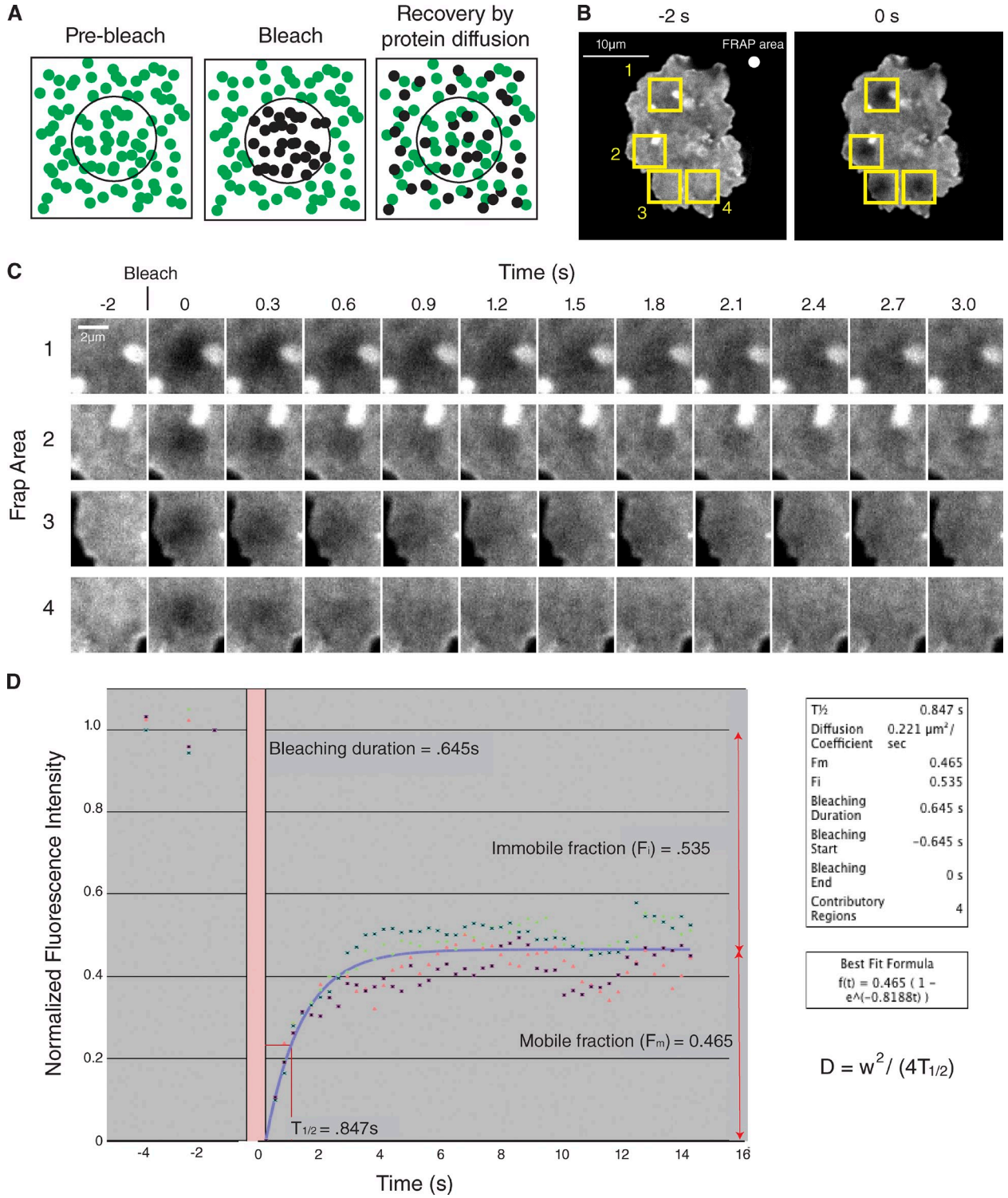

Figure S1. **FRAP methodology.** (A) Cells spreading on coverslips were labeled with fluorescent Fabs, and a small region was photobleached. As bleached (dark) molecules diffuse out, they are replaced by bright molecules from the unbleached regions of the cell, leading to fluorescence recovery. (B) Prebleach and immediate postbleach image of a DC labeled with anti-MHCII Fab, corresponding to Video 1. (C) Time course of fluorescence recovery for each individual FRAP circle shown in B. (D) Representative graph generated using the Volocity FRAP analysis module, with an automatically generated single exponential best fit curve constrained to cross the origin, which is consistent with a single binding site. The fraction of molecules that can participate in exchange between the bleached and unbleached regions is defined as the mobile fraction. This value is essentially a measure of molecules that can move over large distances on the cell surface, as opposed to molecules that are constrained in their mobility, and cannot exchange (immobile fraction). The diffusion coefficient is calculated based upon the half time required to reach maximal recovery ($T_{1/2}$) and the original bleach area diameter (w) using the equation shown. By definition, this value can be calculated only for mobile molecules in the mobile fraction. These data are taken from the FRAP measurements shown in Fig. 1, and are representative of recovery curves from three independent experiments.

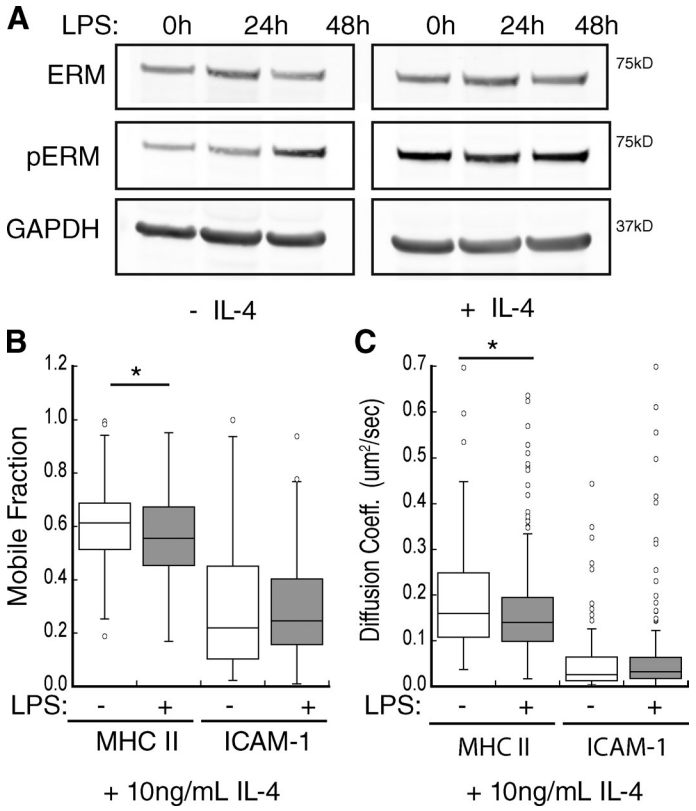

Figure S2. **High-baseline moesin phosphorylation and low ICAM-1 mobility in IL-4 treated BMDCs.** (A) Western blot showing ERM protein expression and phosphorylation in BMDCs cultured in the presence or absence of 10 ng/ml of IL-4, and in the presence or absence of LPS. (B and C) BMDCs were cultured in the presence of 10 ng/ml IL-4 ± LPS for 24 h, and the mobile fraction (B) and diffusion coefficient (C) of ICAM-1 were determined using FRAP analysis. Box plots were created from 55–290 individual FRAP measurements pooled from three independent experiments. *, $P < 0.01$.

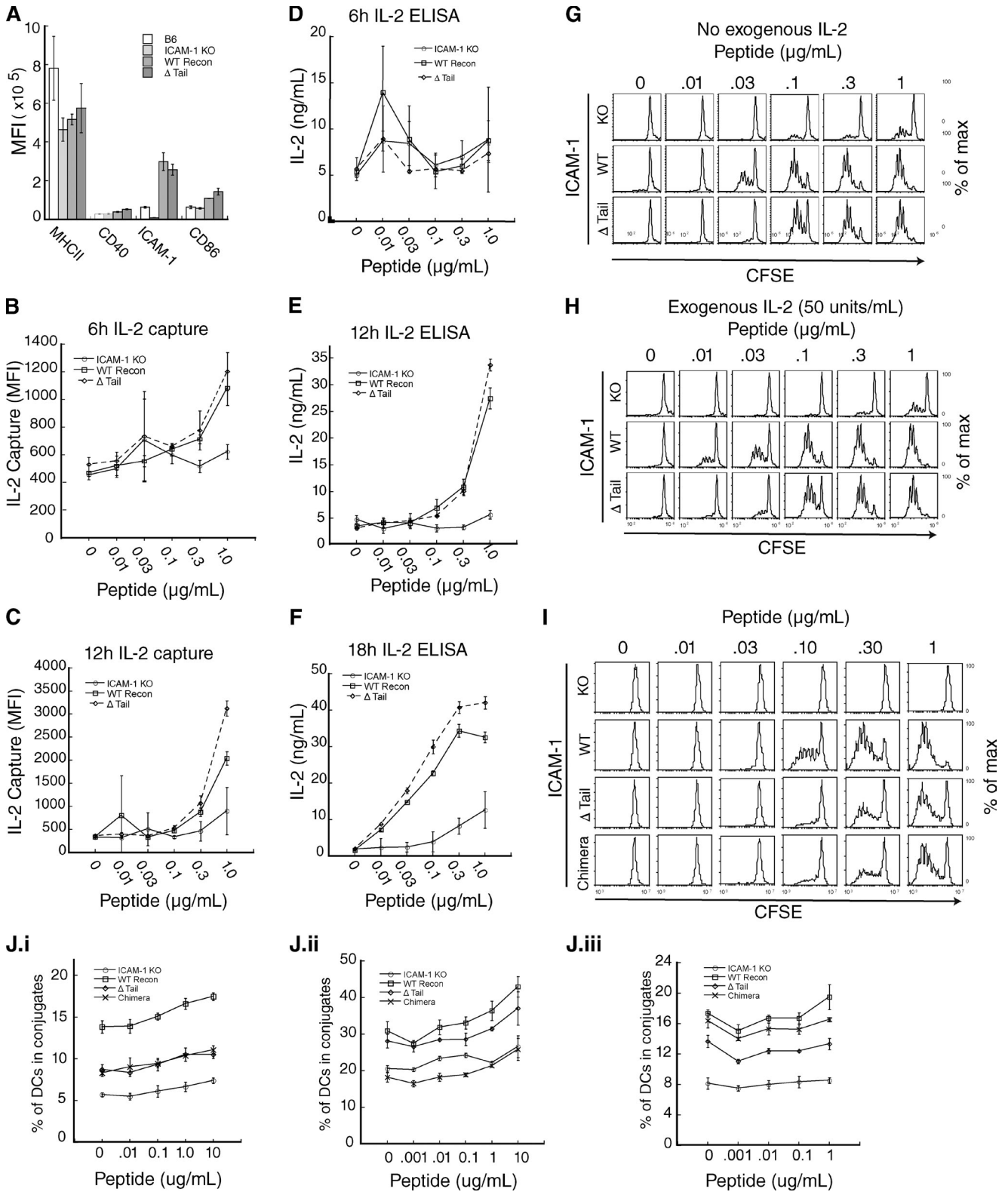

Figure S3. **Mechanistic analysis of defective T cell priming by DCs expressing ICAM-1 mutants with altered mobility.** (A) Control C57BL/6 DCs or ICAM-$1^{-/-}$ DCs transduced as indicated were stimulated with LPS, and surface expression of maturation markers was analyzed by flow cytometry. Mean fluorescence intensities of triplicate wells are shown from one representative experiment. (B and C) ICAM-$1^{-/-}$ DCs were transduced with GFP or the indicated ICAM-1 constructs, pulsed with peptide, and used to prime $CD4^+$ OTII T cells. IL-2 secretion was assessed using a surface capture assay after 6 h (B) or 12 h (C) of stimulation. (D–F) Priming of OTII T cells was performed as in B and C. IL-2 secretion was assessed by ELISA after 6 (D), 12 (E), or 18 (F) h of stimulation. (G and H) T cell proliferation after 96 h of stimulation as measured by CFSE dilution in response to transduced BMDCs pulsed with OVA peptide in the absence (G) or presence (H) of 50 U/ml exogenous IL-2. Plots shown are representative of results from two independent experiments. (I) T cell proliferation, as marked by CFSE dilution, after 96 h of stimulation with ICAM-$1^{-/-}$ BMDCs transduced with GFP (ICAM-1 KO), WT, or chimeric ICAM-1. Plots shown are representative of results from three independent experiments. (J) Three separate conjugation assays demonstrating inconsistent results of chimeric ICAM-1–expressing DCs binding to cognate T cells, in comparison with ICAM-$1^{-/-}$ DCs and ICAM-$1^{-/-}$ DCs expressing WT and ΔTail ICAM-1. Error bars represent standard deviation from three triplicate wells from a single representative experiment ($n = 3$).

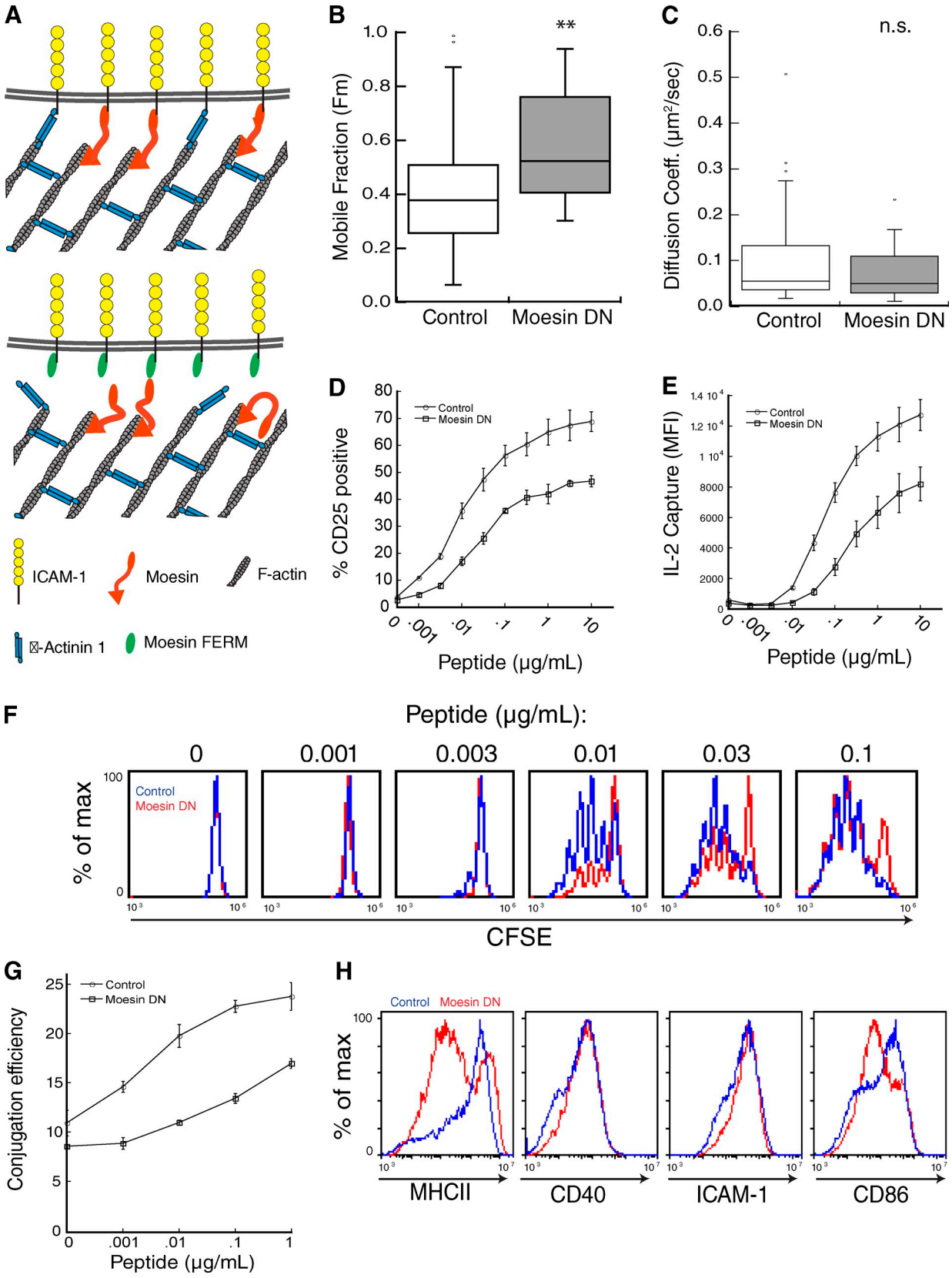

Figure S4. **Overexpression of the moesin FERM domain affects ICAM-1 mobility and T cell priming.** (A) When overexpressed, the FERM domain of moesin can bind the polybasic residue in ERM-interacting partners and prevent interaction with endogenous moesin, and possibly also α-actinin. (B and C) Mobile fraction (B) and diffusion coefficient (C) of ICAM-1 in DCs transduced with either mKATE2 (Control) or Moesin FERM domain fused to mKATE2 (Moesin DN). Box plots were generated from 27–76 FRAP measurements from one experiment, representative of two independent experiments. (D and E) CD25 expression (D) and IL-2 production (E) in OTII T cells responding to DCs transduced as in B and pulsed with the indicated amounts of OVA peptide. (F) Proliferation of OTII T cells responding to transduced DCs. Results are representative of three independent experiments. (G) Conjugation efficiency of T cells interacted with control or moesin DN–transduced DCs. Data in D, E, and G represent means ± standard deviation (error bars) of triplicate wells from a single experiment, representative of three independent experiments. (H) Surface expression of MHCII, CD40, ICAM-1, and CD86 in LPS-matured control or moesin DN-transduced DCs. Results are representative of three independent experiments.

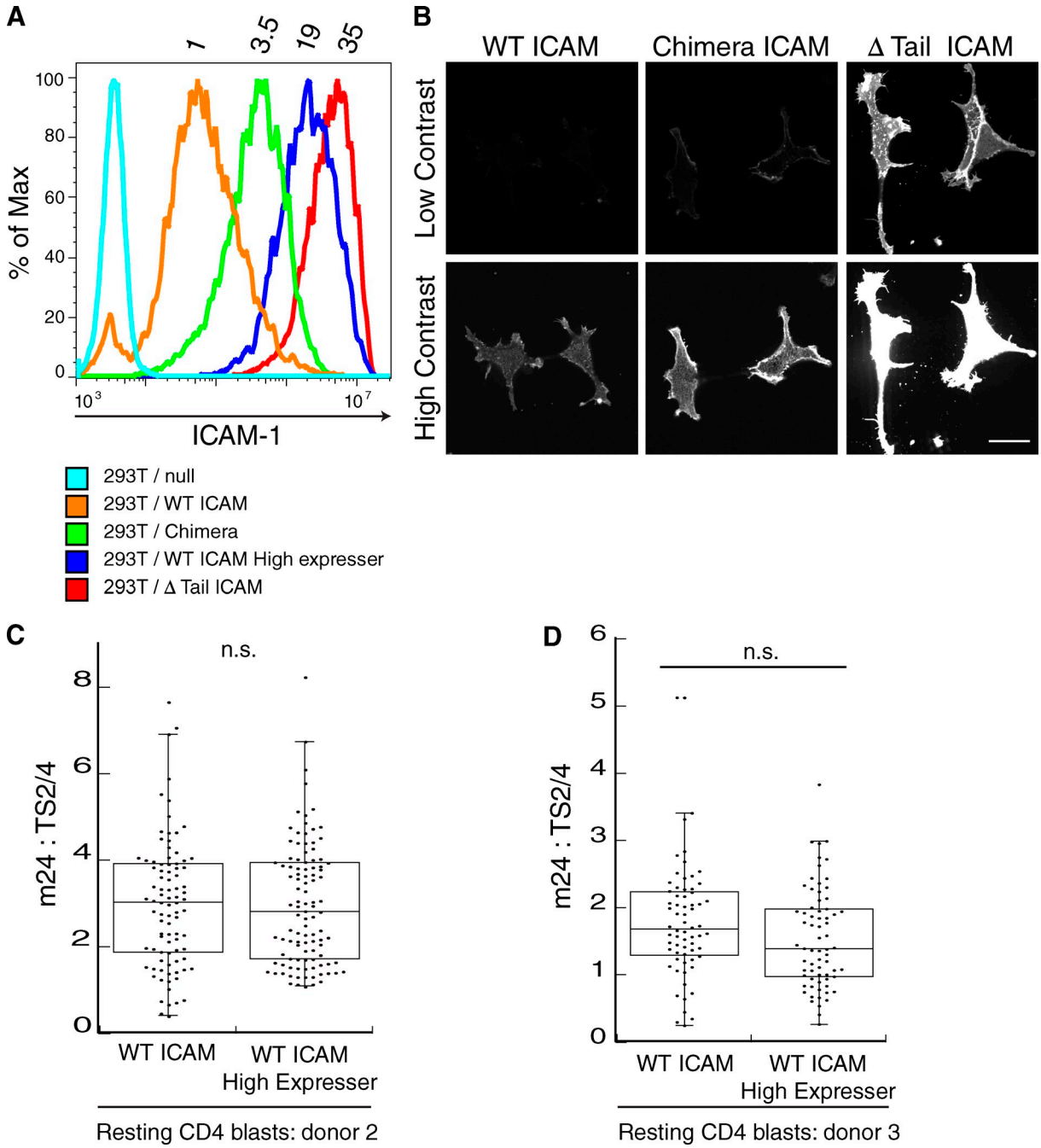

Figure S5. **Conformational change of LFA-1 does not correlate with the expression level of ICAM-1 on artificial APCs.** (A) Flow cytometric analysis showing surface expression of ICAM-1 on the different artificial APCs. Numbers above the peaks represent the mean fluorescence intensity normalized to the WT ICAM clone. Results are representative of two independent experiments. (B) Immunofluorescence images of surface-stained ICAM-1 on 293T cells. Bar, 20 µm. This experiment was completed once, and images are representative of mean ICAM-1 expression. (C and D) Analysis of LFA-1 conformational change on T cells responding to artificial APCs expressing WT ICAM-1 at moderate levels (WT ICAM-1) or at 19-fold higher levels (WT ICAM-1 High expresser). Moderate expressers were used elsewhere throughout the paper; note that data for moderate expressers in C and D are identical to data in Figs. 6 H and 6 I, respectively. These results are pooled from three independent experiments.

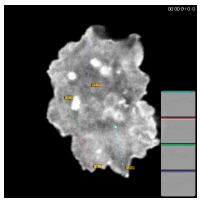

Video 1. **FRAP of MHCII in mature DCs.** LPS-matured BMDCs were allowed to spread on imaging cover glasses and coated with anti-MHCII Fab as detailed in the Materials and methods. FRAP was then conducted with a spinning disk confocal microscope (UltraView; PerkinElmer) and images were collected for 15 s at maximum speed.